Nonlinear Modeling and Comparative Analysis of Damage Mechanisms in ABS: A Study Based on Ultimate Stress and Residual Energy Approaches

Amal Lamarti [1, 2], Abdelilah Hachim [1, 2], Jamila Bouchgl [3, 4], Sara Sandabad [1, 2], Khadija Ouaissa [3,5], Khalid El Had [1, 2]

[1] Higher Institute of Maritimes Studies, Casablanca
[2]Laboratory of Mechanics, Engineering and Innovation, National Higher School of Electricity and Mechanics, Hassan II University of Casablanca (UH2C), Maarif Casablanca 20100, Morocco
[3] Higher Institute of Marine Fisheries, Agadir, Morocco
[4] Laboratory of energy Engineering, Materials and Systems, ENSA, Ibn Zohr University, Agadir, Morocco.
[5]Environmental, Ecological and Agro-Industrial Engineering Laboratory. Department of Biology, Faculty of Sciences and Techniques. University Sultan Moulay Slimane. Beni-Mellal, Morocco.

Abstract. This study takes a closer look at how damage develops in Acrylonitrile Butadiene Styrene (ABS) when it is put under mechanical stress. It compares three different ways to evaluate that damage: one based on how much stress the material can still handle, another based on how much energy it can still absorb, and a third using a unified damage theory. To explore this, researchers tested specially designed samples, with a hole and notches of different lengths, under controlled static loading conditions.

The results revealed a clear three-stage pattern in how damage progresses: it starts slowly (up to $\beta \approx 0.20$), grows steadily (up to $\beta \approx 0.70$), and then accelerates quickly until the material fails. What is particularly interesting is how closely the stress-based and energy-based methods agreed, less than a 5% difference when identifying the critical damage thresholds. This strong correlation suggests these methods are reliable tools for capturing the complex, nonlinear behavior of thermoplastic damage, offering a clear improvement over traditional linear models like Miner's rule.

In the end, this work helps deepen our understanding of how polymers like ABS deteriorate under stress and offers a stronger, more accurate framework for predicting the remaining life of damaged structural parts.

1 Introduction

Assessing damage in polymer materials remains a major challenge for modern engineering, especially when designing structural components exposed to various mechanical loads. Thermoplastic polymers, particularly Acrylonitrile Butadiene Styrene (ABS), are widely used across many industrial applications due to their favorable mechanical properties and ease of processing [20-21] and [44-50]. However, their response to progressive damage is complex and calls for assessment methodologies that are specifically tailored to their microstructural characteristics.

Traditional damage models, such as Miner's rule, are based on a linear accumulation assumption that often falls short when it comes to accurately describing the actual behavior of polymers under load [14, 22]. This limitation has driven the development of more advanced and nuanced approaches ones that incorporate concepts like residual ultimate stresses [19, 24], residual ultimate energies [24, 33], and unified damage theory [13, 16, 25].

The main goal of this study is to compare several damage assessment methods to determine which one best captures the nonlinear way damage evolves in ABS. To do this, we developed an experimental setup using specially designed specimens that include a circular hole and notches of varying lengths. This configuration was chosen to represent different stages of damage and to help us better understand the physical mechanisms at play. In addition, this investigation aims to clarify the precise relationship between accumulated damage and life fraction in thermoplastic polymers [27, 42], to evaluate how closely stress-based and energy-based approaches align [3, 5], and to compare these methods with predictions from both the unified damage theory and Miner's classical linear model [11, 39].
The results are expected to make a meaningful contribution to improving lifetime prediction models for polymer components. These insights could play an important role in refining design criteria and boosting the overall reliability of structural parts used in a variety of industrial applications [2, 4].

2 Experimental methodology

In this section, we describe the polymer material used, the geometry of the test specimens and the experimental procedure followed to capture stress-strain data under mechanical loading. The experiments were carried out in a controlled environment, with the temperature maintained 23°C and humidity levels kept to ensuring stable testing conditions

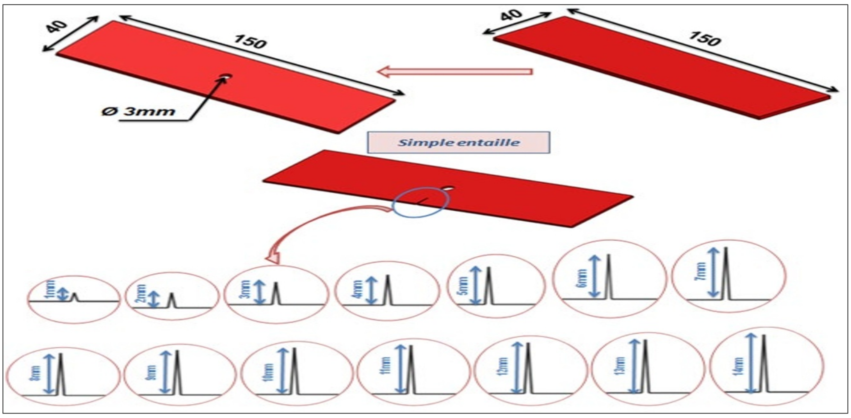

Fig. 1. Steps for Preparing the Combined Defect (Hole and Notch).

In this experiment, we carefully selected specific loading conditions to study how damage develops in Acrylonitrile Butadiene Styrene (ABS). Three different loading types were used to examine how the material behaves under varying stress levels:

- **Load Type:** The tests were carried out using static loading, where force was applied gradually until the material failed. Additionally, quasi-static tests were conducted, involving slow increments of load to mimic extended stress exposure.
- **Loading Speeds**: For the static test, the loading rates were kept deliberately slow to avoid causing rapid fatigue in the material (1,2 mm/min).

- **Notch Geometry**:The samples were designed with a central hole of a constant size, combined with notches of varying lengths (ranging from 0 to 17 mm). This setup was chosen to assess how the size of the defects affects the accumulation of damage, energy absorption, and the material's overall resistance. The length of the notch plays a crucial role in focusing stress, which directly impacts the progression of damage.

Variations in the size and position of notches can lead to differences in experimental results, influencing the material's ability to handle stress and maintain its resilience. Therefore, these geometric defects should be taken into account when assessing the durability and residual energy of the material being tested.

3 Results and discussion

3.1 Nonlinear Damage Evolution According to the Unified Theory: A Comparative Analysis with Miner's Rule

When a material becomes damaged, its endurance limit and static tensile strength both tend to decrease [59]. According to Gatts' hypothesis [60], when the applied stress exceeds the endurance limit, fatigue damage evolves according to a power-law relationship of the form:

$$\gamma_D = \left(\frac{\gamma_{ur}}{\gamma_u}\right)^m \qquad (1)$$

$$\gamma_D = \left(\frac{\sigma_D}{\sigma_{D0}}\right), \gamma_{ur} = \left(\frac{\sigma_{ur}}{\sigma_{D0}}\right), \gamma_u = \left(\frac{\sigma_u}{\sigma_{D0}}\right)$$

Where σ_{D0} is the endurance limit of the undamaged (virgin) material, σ_D is the current endurance limit of the material after *n* loading cycles; σ_{ur} is the current monotonic tensile strength of the material; σ_u is the maximum monotonic tensile strength of the virgin material; m is the empirical constant determined experimentally [36].

Note that, the Bui-Quoc model [37] highlights a connection between monotonic tensile strength and prior cyclic loading. In other words, if a material has undergone repeated loading before a tensile test, its ability to withstand static loads tends to drop [38]. This drop is referred to as a reduction in the material's residual strength [39]: σ_{ur} is the residual ultimate stress of the material after *n* loading cycles, σ_u is the ultimate stress of the undamaged material. β is the life fraction, representing how much of the material's fatigue life has been consumed and $\gamma = \sigma_m/\sigma_{D0}$ represents the loading level, defined as σm, the mean stress during cyclic loading [40].
For polymers, the ultimate stress (σu) is effectively the same as the yield stress (σe) [41]. This means that the parameter *m* is material-specific, and for amorphous polymers, it typically takes the value *m = 1* [42]. The damage model proposed by Bui-Quoc takes a different approach compared to the earlier formulation by Miner [64]:

$$D = \frac{(1-\gamma_D)}{(1-\gamma_D{}^*)} \qquad (2)$$

$\gamma_D = \sigma_D/\sigma_{D0}$ is the endurance limit and $\gamma_D{}^* = \sigma_m/\sigma_{D0}$ is the critical endurance limit.
Many damage theories are rooted in the linear model introduced by Miner's rule, which states that damage increases proportionally with the fraction of life consumed [42].

Based on the idea behind the unified damage theory, a new way to describe damage is suggested. It looks at how the endurance limit of the material gets lower as damage builds up.

$$D = \frac{\beta}{\beta+(1-\beta)\left(\frac{\gamma-\left(\frac{\gamma}{\gamma u}\right)^{m}}{\gamma-1}\right)} \qquad (3)$$

Where β is the life fraction, and determined by the size of the combined defect (the hole and the notch) in relation to the width of the specimen. Specifically, it's the ratio a/w, where a is the length of the notch or hole, and **w** is the width of the material being tested. Furthermore, $\gamma = \sigma_{ur}/\sigma_0$ et $\gamma_u = \sigma_u/\sigma_0$ and m=1 for amorphous polymer [27, 42]. σ_0 is refers to the residual endurance limit, it represents the baseline stress level before damage begins. It is calculated by multiplying the undamaged ultimate stress (σ_u) by a coefficient α for (n=0 and $\sigma_0=\alpha \times \sigma u$). For $\alpha = (the\ safety\ factor\ of\ an\ amorphous\ polymer)^{-1}$, figure 2 shows the evolution of damage, calculated using the unified damage theory (Equation 3), as a function of the life fraction β for specimens that were pre-damaged. The curves corresponding to different γ values (1.01, 1.24 and 1.91) illustrate how the material behaves under various loading levels, compared to Miner's linear rule, represented by the green line [11, 42].

The analysis reveals that as γ increases, the damage curves deviate more noticeably from linearity. In contrast, under higher loading levels (i.e., lower γ values), the damage curve gradually approaches the bisector line that represents Miner's rule. This convergence toward linear behavior is more

pronounced as the life fraction β increases. This behavior showed that the level of loading plays an important role in how damage develops over time [15, 16, 25].

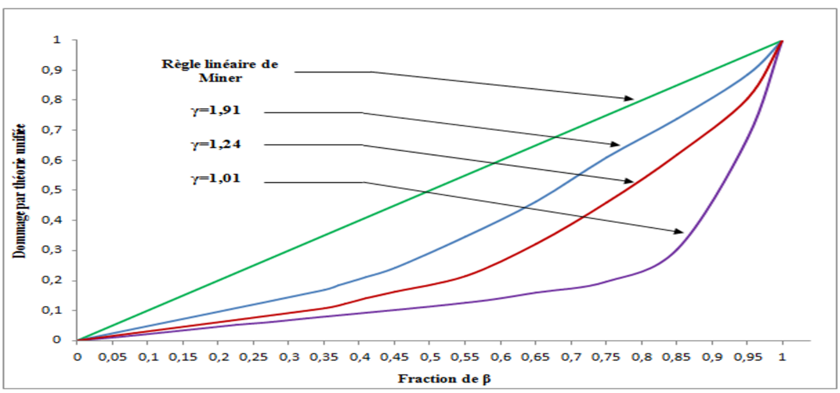

Fig. 2. Characteristic curves showing damage as a function of life fraction β, based on the unified theory, for specimens with holes and single notches.

3. 2 Comparison of experimental and theoretical damage quantification approaches

Figure 3 presents a comparative analysis of how damage evolves with respect to the life fraction β, using three distinct methods.

The curves illustrate experimental static damage (Ds, in blue), damage calculated using the unified theory (Dthe unified, in green) and the prediction from Miner's linear rule (in red) [11, 42]. This comparison allows for a quantitative evaluation of damage in ABS and provides a solid basis for comparing theoretical approaches with experimental results [9, 10]. We observe that experimental static damage increases rapidly at low life fraction, reaching 0.5 as early as β = 0.3. In contrast, the unified theory predicts a more conservative, nonlinear progression that starts slowly and accelerates toward the end of life of the material [17, 25].

Miner’s rule, on the other hand, maintains a strictly linear progression that falls between the two behaviors.

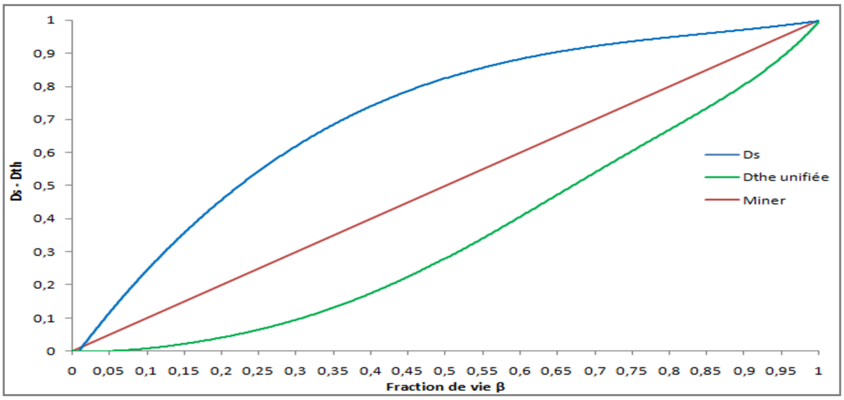

Fig. 3. Comparison of Damage Evolution Based on Static Damage, Unified Theory, and Miner’s Rule as a Function of Life Fraction

The curve shows a strong correlation between the experimental static damage (Ds) and the damage predicted by the unified theory; with both showing, an overall increasing trend as the life fraction β increases. However, a gap appears between the two, especially in the mid-range values of β. The experimental static damage tends to rise more quickly during the early and middle stages of the material's life, while the unified theory predicts a more conservative progression that accelerates mainly toward the end [22, 23].
Miner’s linear rule falls somewhere in between these two behaviors, following a steady progression that overestimates damage compared to the unified theory, but underestimates the damage observed experimentally across most of the material’s life span [11, 42].
This triangular configuration of the three curves clearly illustrates the limitations of purely theoretical models in accurately capturing real-world damage mechanisms in polymer materials like ABS [44-50].

3.3 Damage evaluation using an energy based approach

This section aims to identify key material parameters that can be used to quantitatively predict the risk of sudden failure in components containing defects. An energy-based damage evaluation approach is applied to ABS specimens containing a combined defect, a circular hole with a constant diameter, paired with notches of varying lengths [33].
The total energy of the material must be determined by integrating the full stress. This total energy includes the energy used to initiate damage and the energy needed to propagate the crack through the remaining ligament, as noted in the literature.

3.3.1 Total Energy Analysis

From a physical point of view, damage in a material can be seen through several signs [40, 41]:

- A decrease in residual strength [19, 24]
- A reduction in the endurance limit [9, 10]
- An increase in the stress applied to the damaged area [1, 3]
- A loss of energy during the material’s deformation [33, 43]

The ultimate energy method is used to describe how damage progresses in test specimens with holes and notches during static loading. It works by measuring the amount of energy the material absorbs up to the point of failure [24, 33]. This energy is calculated by finding the area under the stress–strain curve using numerical integration.
To compute the total energy, a step-by-step method is used that adds up the small areas between each pair of data points ($d\sigma \times d\varepsilon$). This technique breaks the full curve into smaller sections, and their sum gives a precise estimate of the energy that was dissipated during the test.
Figure 4 shows how the total energy absorbed by the specimen increases or decreases as the notch length changes, with the constant central hole diameter.
The graph shows how the total energy (W), in joules, changes with the size of the defect (a hole and a notch), measured in millimeters. The curve adds up the energy used for each notch length. At each stage of the test, each life fraction β, the total energy is calculated by combining the energy used as the notch gets longer.

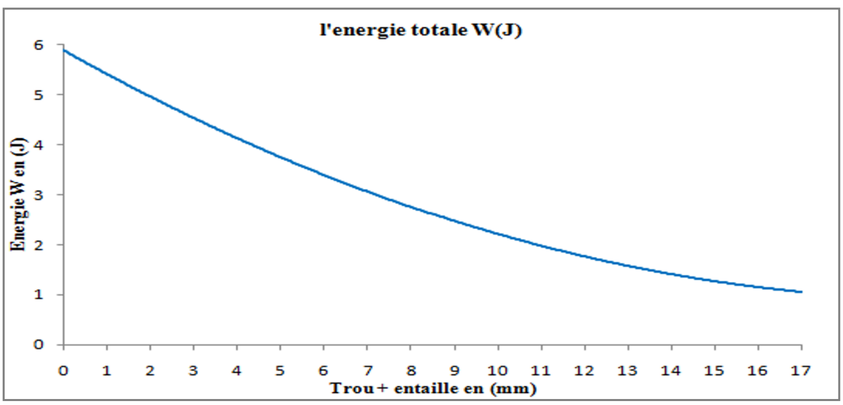

Fig. 4. Total energy comparison for ABS specimens with notch and hole defects

A clear negative correlation can be seen: as the notch length increases (from 0 to 17 mm), the total energy of the specimen drops significantly (from about 6 J to 1 J). This drop in energy happens because the growing defect causes higher stress in a small area, which lowers the material's ability to absorb energy through plastic deformation [30]. As the defect grows, the material slowly loses its ability to stretch or deform, which leads to a decrease in the total plastic energy stored in the specimen.

3.3.2 Loss of residual ultimate energy

The loss of residual ultimate energy is an important parameter for evaluating how a material degrades over time under stress [24, 33]. This value shows how the material is ability to absorb energy decreases, as it gets closer to final failure.
Figure 5 presents a clear summary of the energy values related to each drop in stress recorded during standard static tests. The experimental values appear on a graph as a function of β, the life fraction of the material. This helps place the deterioration process on a normalized timeline.
The curve analysis shows a clear decreasing trend in the residual ultimate energy loss (Uur) as the material progresses through its life fraction. The energy loss is much higher in the early stages of the material's life (when β is close to 0), then drops sharply and follows an exponential decline until it reaches a stable plateau around $\beta = 0.55$ [18, 33]. Beyond this critical point, the residual energy remains extremely low until the specimen completely fails.

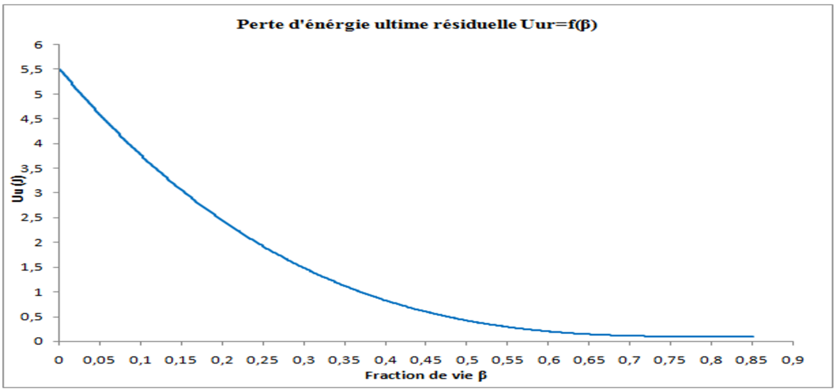

Fig. 5. Energy loss in damaged specimens with different notch lengths under static tension

This behavior suggests that once the material reaches around 60% of its life, only a relatively small amount of energy is needed to cause final failure [43].
Note that, from here on, we will use the maximum energy as a key reference to build a static damage model based on the energy approach [24, 33].

3.3.3 Energy damage and evaluation of material degradation

The main goal of this methodological approach is to provide a rigorous quantification of the damage experienced by thermoplastic polymer specimens, based on the analysis of the energy dissipated up to final failure [33, 43]. This method enables a precise characterization of the gradual deterioration of the material's mechanical properties.
To systematically assess the accumulated damage in energy terms, we developed a contribution to the static damage model, calculated from the residual ultimate energy "Ds." The mathematical expression and graphical representation of this model are shown in Figure 6, in line with previous studies [42].

$$D_{enrg} = \frac{1-\frac{U_{ur}}{U_u}}{1-\frac{U_a}{U_u}} \tag{4}$$

With U_{ur} is the residual ultimate energy of the damaged material, U_u is the ultimate energy of the virgin material and U_a is the applied energy just before failure.
The boundary conditions are:

- at the initial state: $\beta = 0$, $U_{ur} = U_u$, $D = 0$.
- at the final state: $\beta = 1$, $Uur = Ua$, $D = 1$.

Figure 6 shows how energy-based damage (D_{enrg}) changes with the life fraction (β) in specimens with holes and notches under mechanical loading. The curve shows a nonlinear relationship, which is typical of how the material breaks down over time [24, 33]. It can be seen that the cohesive energy stored in the material slowly decreases as the notch length increases. This leads to a clear drop in the material's resistance to crack growth [5, 30, 31].
The curve shows three phases in the damage process. After an initial damage stage that reaches about β = 20%, the material starts to degrade much faster and enters a phase of growing instability [32, 43]. This instability peaks during the acceleration phase, which

becomes very noticeable around β = 65%. At this critical point, the damage becomes sudden and severe.

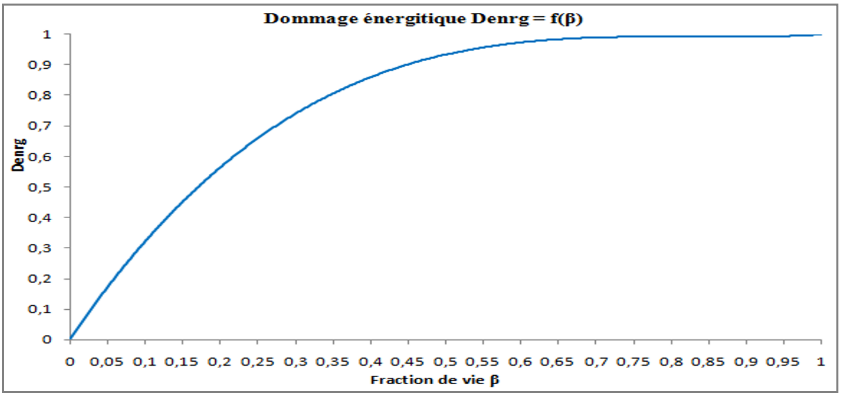

Fig. 6. Residual Energy-Based Damage Evolution as a Function of Life Fraction

3.3.3 Damage reliability based on the energy method (Denrg - Renrg)

The simultaneous analysis of damage and reliability represents a fundamental approach for characterizing the evolution of the structural state of thermoplastic materials under stress [2, 4]. Reliability 'R', defined as the probability of the material's survival, follows a mathematically decreasing function that evolves inversely with the accumulated damage, in accordance with the following relationship:

$$R_{enrg} + D_{enrg} = 1 \qquad (4)$$

This fundamental equation enabled us to graphically establish the correlation between residual reliability and the previously studied energy-based damage. The application of the energy method proved particularly relevant for accurately identifying the three characteristic stages of material evolution, marked by the intersection points of the damage and reliability curves, as illustrated in Figure 7 [22, 24].

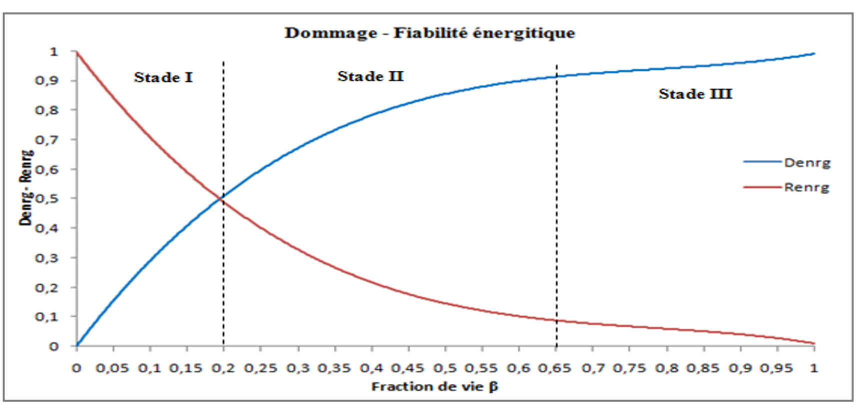

Fig. 7. Superposition of Static Damage and Static Reliability Curves as a Function of Life Fraction

A thorough analysis of Figure IV.8, which shows the interaction between the damage (Denrg) and reliability (Renrg) curves, allows us to identify and characterize three distinct stages in the material degradation process [22, 24, 33]:

- Stage I [0–20%]: This initial phase corresponds to the damage initiation zone, clearly marked by the first intersection of the Damage-Reliability curves at β = 20%. During this period, the material maintains a reliability level higher than the accumulated damage, indicating its ability to preserve its mechanical properties despite the early signs of degradation.
- Stage II [20%–65%]: This middle phase reflects a steady yet notable progression of damage, accompanied by a proportional decrease in reliability. At β = 65%, which marks the end of this stage, a sharp acceleration in the damage process occurs, signaling the onset of a critical condition in the material [23].
- Stage III [65%–100%]: This final phase, beginning at 65% of the life fraction, is marked by sudden and irreversible damage. By analogy with crack propagation mechanisms, entering this stage corresponds to the onset of structural instability, which inevitably leads to the complete failure of the material.

Note that, using β and damage curves helps define safety and inspection/maintenance criteria based on how damage progresses. These guidelines ensure that timely interventions are made to manage the material's durability before failure risks escalate.

3.3.3 Quantification of Energy-Based Damage Using the Unified Theory

The energy-based damage quantification approach grounded in the unified theory represents a significant advancement over traditional linear models [13, 16, 25]. By incorporating the intrinsic parameters of materials, this methodology offers a more accurate depiction of the complex mechanisms behind progressive degradation. Based on the fundamental Equation 4 of the unified theory, we developed a comparative model of cumulative damage. The experimental results obtained through this theoretical approach are presented graphically in Figure 8, allowing for a direct comparison with the predictions of Miner's classical linear model [11, 39].

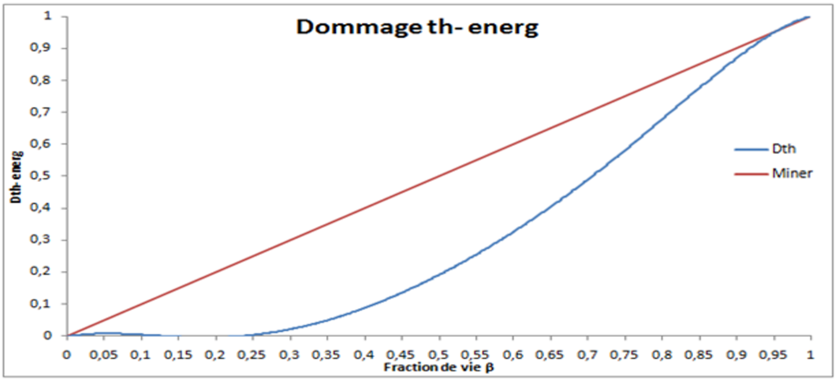

Fig. 8. Characteristic curves representing damage as a function of the life fraction β, based on the unified theory, for notched and drilled specimens.

The comparative analysis of the curves shown in Figure 8 reveals fundamental differences between the two damage quantification approaches. Miner's model produces a strictly linear progression of damage with respect to the life fraction, following a direct proportional relationship [11, 39]. In contrast, the damage calculated using the unified theory exhibits a clearly nonlinear evolution, characterized by two distinct phases: an initial moderate increase up to a critical life fraction of approximately 40%, followed by a substantial acceleration of degradation leading to the final failure of the specimen [13, 25].

This significant divergence between the two models highlights the inherent limitations of Miner's rule for this specific category of materials [14, 22]. The inadequacy of the linear model stems mainly from its mathematical formulation, which relies primarily on geometric parameters, particularly the ratio between the instantaneous crack length (a_1) and the total length at failure (a_t). This approach fails to account for the intrinsic properties of the material that fundamentally govern its mechanical behavior.
In contrast, the unified theory incorporates fundamental material parameters such as the ultimate stress and the endurance limit of the virgin material, thus providing a more realistic representation of the physical degradation mechanisms [13, 16, 17]. This ability to account for the intrinsic properties of the material gives the nonlinear model greater relevance for predicting the actual behavior of thermoplastic specimens subjected to progressively applied mechanical stresses.

4 Conclusion

This research established an in-depth comparison between various damage evaluation methodologies applied to Acrylonitrile Butadiene Styrene (ABS) subjected to mechanical loading. The analysis of experimental results revealed several key insights into the behavior of this thermoplastic polymer under progressive damage.

First, the study clearly demonstrated the nonlinear nature of damage evolution with respect to the life fraction, thereby challenging the applicability of Miner's linear rule for this class of materials. The three methodological approaches, based on residual ultimate stress, residual energy, and the unified theory, converged toward a similar characterization of the damage process, identifying three distinct phases: an initiation phase (up to $\beta \approx 0.20$), a progressive propagation phase (up to $\beta \approx 0.65$), and a phase of rapid acceleration leading to failure.

Second, the comparison between experimental results and theoretical predictions highlighted the importance of incorporating fundamental material parameters, such as ultimate stress and endurance limit, into damage prediction models. This integration enables a more accurate description of the physical mechanisms governing the degradation of the material's mechanical properties.
Third, the energy-based analysis made it possible to precisely quantify the progressive loss of the material's energy absorption capacity as damage advanced. This approach proved especially relevant for identifying critical thresholds that mark transitions between the different phases of damage.

The intersection of the damage and reliability curves at $\beta \approx 0.65$ stands out as a key finding of this study, indicating the point at which the material enters an irreversible phase of structural instability. This observation has direct implications for defining safety criteria in the design of ABS structural components.

Looking ahead, this work opens up several promising research directions, including extending this comparative methodology to other families of thermoplastic polymers, exploring the influence of environmental conditions on damage processes, and developing predictive models that incorporate the effects of load history on damage evolution.

In conclusion, this study makes a significant contribution to improving our understanding of damage mechanisms in thermoplastic polymers and provides a robust methodological framework for assessing the residual lifetime of structural components with defects. A further point is that mold design, additives, and the type of ABS used all play a crucial role in determining factors like β (life fraction) and residual energy. Mold imperfections can introduce internal stresses, while additives can change the material's strength and flexibility.

Additionally, different grades of ABS, whether impact-resistant or heat-resistant, offer varying degrees of toughness and energy absorption. These factors all influence how ABS behaves under stress and how it degrades over time.
The results of this study can be applied to other thermoplastics, but with caution. ABS has its own unique properties, and other materials like polycarbonate or nylon may behave differently due to their molecular structures. The damage mechanisms and models used in this study can be adapted to other polymers, but each one will need its own validation. Additionally, environmental factors like temperature and humidity can affect materials in different ways. In short, while the methodology can be applied, further studies are needed for each polymer to ensure the results are relevant [51].

References

1. Lemaitre J, Chaboche JL. Mécanique des matériaux solides. 3e édition. Paris: Dunod; 2009.
2. Kachanov LM. Introduction to continuum damage mechanics. Boston: Martinus Nijhoff Publishers; 1986.
3. Krajcinovic D. Damage mechanics. Amsterdam: Elsevier; 1996.
4. Voyiadjis GZ, Kattan PI. Advances in damage mechanics: metals and metal matrix composites. Amsterdam: Elsevier; 1999.
5. Chudnovsky A, Shulkin Y. Application of the crack layer theory to modeling of slow crack growth in polyethylene. International Journal of Fracture. 1999;97(1-4):83-102.
6. Lesser AJ. Changes in mechanical behavior and fracture during fatigue of engineering thermoplastics. Polymer Engineering & Science. 1995;35(10):835-840.
7. Petiniot JL, Meo S. Damage evaluation in ABS components using ultrasonic and thermal methods. Polymer Testing. 2002;21(3):333-340.
8. Masaki H, Ogawa H. Fatigue behavior of polymers as structural materials. Journal of Materials Science. 1992;27(20):5447-5456.
9. Bathias C, Pineau A. Fatigue of materials and structures. London: ISTE Ltd and John Wiley & Sons; 2010.
10. Suresh S. Fatigue of materials. 2nd ed. Cambridge: Cambridge University Press; 1998.
11. Miner MA. Cumulative damage in fatigue.
12. Journal of Applied Mechanics. 1945;12(3):159-164[12] Gatts RR. Application of a cumulative damage concept to fatigue. Journal of Basic Engineering. 1961;83(4):529-540.
13. BuiQuoc T, Dubuc J, Bazergui A, Biron A. Cumulative fatigue damage under stress-controlled conditions. Journal of Basic Engineering. 1971;93(4):691-698.
14. Manson SS, Halford GR. Practical implementation of the double linear damage rule and damage curve approach for treating cumulative fatigue damage. International Journal of Fracture. 1981;17(2):169-192.
15. Starke P, Walther F, Eifler D. New fatigue life calculation method for quenched and tempered steel SAE 4140. Materials Science and Engineering: A. 2009;523(1-2):246-252.
16. Chaboche JL. Continuous damage mechanics — A tool to describe phenomena before crack initiation. Nuclear Engineering and Design. 1981;64(2):233-247.
17. Lemaitre J. A continuous damage mechanics model for ductile fracture. Journal of Engineering Materials and Technology. 1985;107(1):83-89.

18. Tao G, Xia Z. An experimental study of uniaxial fatigue behavior of an epoxy resin by a new noncontact real-time strain measurement and control system. Polymer Engineering & Science. 2007;47(6):780-788.
19. Yang JN, Liu MD. Residual strength degradation model and theory of periodic proof tests for graphite/epoxy laminates. Journal of Composite Materials. 1977;11(2):176-203.
20. Hamed GR, Zhao J. Tensile behavior of styrene-butadiene block copolymers containing styrene domains of controlled size. Polymer. 1999;40(14):4103-4112.
21. Ramsteiner F, Armbrust T. Fatigue crack growth in polymers. Polymer Testing. 2001;20(3):321-327.
22. Hwang W, Han KS. Cumulative damage models and multi-stress fatigue life prediction. Journal of Composite Materials. 1986;20(2):125-153.
23. Shirazi A, Varvani-Farahani A. A stiffness degradation based fatigue damage model for FRP composites of (0/θ) laminate systems. Applied Composite Materials. 2010;17(2):137-150.
24. Reifsnider KL, Case SW. Damage tolerance and durability of material systems. New York: Wiley-Interscience; 2002.
25. Chaboche JL, Lesne PM. A non-linear continuous fatigue damage model. Fatigue & Fracture of Engineering Materials & Structures. 1988;11(1):1-17.
26. Shojaei AK, Li G. Viscoplasticity analysis of semicrystalline polymers: A multiscale approach within micromechanics framework. International Journal of Plasticity. 2013;42:31-49.
27. Lesser AJ. Fatigue behavior of polymers. In: Encyclopedia of Polymer Science and Technology. New York: John Wiley & Sons, Inc.; 2002.
28. Avanzini A. Effect of cyclic strain on the mechanical behavior of virgin and recycled polypropylene. Journal of Applied Polymer Science. 2011;122(6):3559-3570.
29. Brinson HF, Brinson LC. Polymer engineering science and viscoelasticity. New York: Springer; 2008.
30. Ritchie RO. Mechanisms of fatigue crack propagation in metals, ceramics and composites: Role of crack tip shielding. Materials Science and Engineering: A. 1988;103(1):15-28.
31. Friedrich K, Walter R, Voss H, Karger-Kocsis J. Effect of short fibre reinforcement on the fatigue crack propagation and fracture of PEEK-matrix composites. Composites. 1986;17(3):205-216.
32. Lang RW, Stern A, Doerner G. Applicability and limitations of current lifetime prediction models for thermoplastics pipes under internal pressure. Angewandte Makromolekulare Chemie. 1997;247(1):131-145.
33. Sauer JA, Richardson GC. Fatigue of polymers. International Journal of Fracture. 1980;16(6):499-532.
34. Tao G, Xia Z. A non-contact real-time strain measurement and control system for multiaxial cyclic/fatigue tests of polymer materials by digital image correlation method. Polymer Testing. 2005;24(7):844-855.
35. Gatts RR. Cumulative fatigue damage with random loading. Journal of the Aerospace Sciences. 1962;29(1):76-80.
36. Marco SM, Starkey WL. A concept of fatigue damage. Transactions of the ASME. 1954;76:627-632.
37. Buiquoc T. An engineering approach for cumulative damage in metals under creep loading. Journal of Engineering Materials and Technology. 1979;101(4):337-343.
38. Lemaitre J, Plumtree A. Application of damage concepts to predict creep-fatigue failures. Journal of Engineering Materials and Technology. 1979;101(3):284-292.

39. Miner MA. Cumulative damage in fatigue. Journal of Applied Mechanics. 1945;12(3):159-164.
40. Chaboche JL. Time-independent constitutive theories for cyclic plasticity. International Journal of Plasticity. 1986;2(2):149-188.
41. Boyce MC, Parks DM, Argon AS. Large inelastic deformation of glassy polymers. Part I: Rate dependent constitutive model. Mechanics of Materials. 1988;7(1).
42. Xiao C, Jho JY, Yee AF. Correlation between the shear yielding behavior and secondary relaxations of bisphenol A polycarbonate and related copolymers. Macromolecules. 1994;27(10):2761-2768.
43. Kinloch AJ, Young RJ. Fracture behaviour of polymers. London: Applied Science Publishers; 1983.
44. Bennis, H., Elkori, R., Hachim, A., Had, K. E., Maliki, A. E., & Sandabad, S. (2025). Determining the impact of accelerated hydrothermal aging on the mechanical properties of polyvinyl chloride and chlorinated polyvinyl chloride. Journal of Polymer Research, 32(2), 1-8.
45. Elkori. R.. Lamarti. A.. Had. K. E.. & Hachim. A. (2022). Experimental Analysis of Ductile–Brittle Change in High-density Polyethylene Behavior. In Recent Advances in Structural Engineering and Construction Management: Select Proceedings of ICSMC 2021 (pp. 131-139). Singapore: Springer Nature Singapore.
46. Elkori. R.. Lamarti. A.. Salmi. H.. Hachim. A.. & El had. K. (2023). Degradation of high-density polyethylene packaging by accelerated aging in sea water. Polymer Engineering & Science. 63(7). 2241-2250.
47. Elkori. R.. Lamarti. A.. Salmi. H.. Had. K.. & Hachim. A. (2024). Experimental study of the degradation of HDPE packaging under accelerated thermal aging. Engineering Solid Mechanics. 12(2). 195- 206.
48. Elkori. R.. Baha. M.. Hachim. A.. Elhad. K.. & Lamarti. A. (2021. April). Comparison of the mechanical behavior of two thermo-plastic polymers by static tests (numerically and experimentally): High- Density Polyethylene (HDPE) and High Impact Polystyrene (HIPS). In Proceedings of the 4th International Conference on Networking. Information Systems & Security (pp. 1-5).
49. Elkori, R., Lamarti, A., El Had, K., & Hachim, A. (2024). Investigation of amyl acetate sorption impact on high-density polyethylene bottle properties. Polymer International.
50. Elkori. R.. Lamarti. A.. Salmi. H.. Hachim. A.. & El Had. K. (2023). Failure behavior of high-density polyethylene and high impact polystyrene: An experimental study by damage methods. Polyolefins Journal. 10(3). 127-136.
51. Fucikova, K., Ovsik, M., Cesnek, A., Pis, A., Vanek, J., & Stanek, M. (2025). Influence of Injection Molding Parameters and Distance from Gate on the Mechanical Properties of Injection-Molded Polypropylene. *Polymers*, *17*(8), 1012. https://doi.org/10.3390/polym17081012